

See discussions, stats, and author profiles for this publication at: <https://www.researchgate.net/publication/51400201>

Synthesis, Characterization, Antioxidant Activity and DNA-Binding Studies of Three Rare Earth (III) Complexes with 1-(4-Aminoantipyrine)-3-tosylurea Ligand

ARTICLE in JOURNAL OF FLUORESCENCE · JANUARY 2009

Impact Factor: 1.93 · DOI: 10.1007/s10895-008-0381-7 · Source: PubMed

CITATIONS

24

READS

98

7 AUTHORS, INCLUDING:



Zhi-hong Xu

Xuchang University

31 PUBLICATIONS 445 CITATIONS

SEE PROFILE



Zheng-zhi Zeng

Lanzhou University

32 PUBLICATIONS 377 CITATIONS

SEE PROFILE

Synthesis, Characterization, Antioxidant Activity and DNA-Binding Studies of Three Rare Earth (III) Complexes with 1-(4-Aminoantipyrine)-3-tosylurea Ligand

Pin-xian Xi · Zhi-hong Xu · Xiao-hui Liu ·
Feng-juan Chen · Zheng-zhi Zeng · Xiao-wen Zhang ·
Ying Liu

Received: 9 March 2008 / Accepted: 30 April 2008 / Published online: 4 June 2008
© Springer Science + Business Media, LLC 2008

Abstract 1-(4-Aminoantipyrine)-3-tosylurea (H_2L) and its three lanthanide (III) complexes, $M(H_2L)_3 \cdot 3NO_3$ [where $M=Nd(III)$, $Sm(III)$ and $Eu(III)$], have been synthesized and characterized. In addition, the DNA-binding properties of the three complexes have been investigated by UV–vis (ultraviolet and visible) absorption spectroscopy, fluorescence spectroscopy, circular dichroism (CD) spectroscopy, cyclic voltammetry, and viscosity measurements. Results suggest that the three complexes bind to DNA via a groove binding mode. Furthermore, the antioxidant activity (super-oxide and hydroxyl radical) of the metal complexes was determined by using spectrophotometer methods in vitro. These complexes were found to possess potent antioxidant activity and be better than standard antioxidants like vitamin C and mannitol.

Keywords 1-(4-Aminoantipyrine)-3-tosylurea ·
Rare earth (III) complex · Groove binding ·
Antioxidant activity

Introduction

Sulfonylurea derivatives are the most widely prescribed drugs for the treatment of the maturity onset form of diabetes mellitus [1–4], and many of their ramifications had been used as herbicide [5, 6] and anticancer [7, 8]. The metal complexes of sulfonylurea also have many noticeable bioactivities [9]. The synthesis of the complexes of sulfonylurea plays an important role in researching the co-operation between the metal ions and the ligand and exploring the mechanism of the molecular biology [10]. Investigation on molecular complexes of lanthanide ions has been attracted significant attention, owing to their fluorescent broad applications in biochemistry, material chemistry, medicine and so forth [11–13]. Yet it is noticed that the DNA-binding investigation of such complexes have been relatively few. We have previously reported [14] on the synthesis and characterization of several lanthanide complexes with sulfonylurea ligands. In light of our research, we have concluded that the precise nature of the ligands is of remarkable importance in the interaction of the complex with the DNA molecule. Therefore, extensive studies with different structural ligands are necessary in order to understand and evaluate the factors that determine both the DNA-binding mode and the biological activity of their complexes.

However, up to now the biological activity and interactions of 4-aminoantipyrine and ethyl *N*-(3-tosylsulfonyl) carbamate and their complexes with DNA have not been reported. This aroused our interest in synthesis of a new ligand 1-(4-aminoantipyrine)-3-tosylurea, and its $Nd(III)$, $Sm(III)$ and $Eu(III)$ complexes in view of evaluating their pharmaceutical activities.

P.-x. Xi · Z.-h. Xu · X.-h. Liu · F.-j. Chen · Z.-z. Zeng (✉)
State Key Laboratory of Applied Organic Chemistry and College
of Chemistry and Chemical Engineering, Lanzhou University,
Lanzhou 730000, People's Republic of China
e-mail: zengzhzh@yahoo.com.cn

X.-w. Zhang · Y. Liu
Gansu Academy of Medical Sciences,
Lanzhou 730050, People's Republic of China

Experimental section

Materials and physical measurements

All reagents and solvents were purchased commercially and used without further purification unless otherwise noted. Calf thymus DNA (CT-DNA) was obtained from Sigma Chemicals Co. (USA) and used as received. Solutions of CT-DNA in 50 mM NaCl, 5 mM Tris–HCl (tris(hydroxymethyl)aminomethane hydrochloride) (pH 7.2) gave a ratio of UV–Vis absorbance of 1.8–1.9:1 at 260 and 280 nm, indicating that the DNA was sufficiently free of protein [15]. The concentration of DNA was determined spectrophotometrically using a molar absorptivity of $6,600 \text{ M}^{-1} \text{ cm}^{-1}$ (260 nm) [16]. Double-distilled water was used to prepare buffers.

Carbon, hydrogen, and nitrogen were analyzed on an Elemental Vario EL analyzer. Infrared spectra ($4,000\text{--}400 \text{ cm}^{-1}$) were determined with KBr disks on a Thermo Mattson FTIR spectrometer. The UV–visible spectra were recorded on a Varian Cary 100 UV–Vis spectrophotometer. ^1H NMR spectra were measured on a Varian VR 300-MHz spectrometer, using TMS as a reference in DMSO- d_6 . Mass spectra were performed on a VG ZAB-MS (FAB) instrument and electrospray mass spectra (ESI-MS) were recorded on a LQC system (Finnigan MAT, USA) using CH_3OH as mobile phase.

Absorption titration experiment was performed with fixed concentrations of the drugs, while gradually increasing concentration of DNA. While measuring the absorption spectra, an equal amount of DNA was added to both compound solution and the reference solution to eliminate the absorption of DNA itself. In order to compare quantitatively the binding strength of the three complexes, the intrinsic binding constants K_b of the three complexes with DNA were obtained by monitoring the changes in absorbance at 205 nm for the complex **1**, complex **2** and **3** with increasing concentration of DNA using the following equation [17]:

$$[\text{DNA}]/(\varepsilon_a - \varepsilon_f) = [\text{DNA}]/(\varepsilon_b - \varepsilon_f) + 1/K_b(\varepsilon_b - \varepsilon_f) \quad (1)$$

where $[\text{DNA}]$ is the concentration of DNA in base pairs, the apparent absorption coefficient ε_a , ε_f and ε_b correspond to $A_{\text{obsd}}/[\text{M}]$, the extinction coefficient of the free compound and the extinction coefficient of the compound when fully bound to DNA, respectively. In plots of $[\text{DNA}]/(\varepsilon_a - \varepsilon_f)$ versus $[\text{DNA}]$, K_b is given by the ratio of slope to the intercept.

Fluorescence spectra were recorded on a Hitachi RF-4500 spectrofluorophotometer. Fixed amounts (10 μM) of the complexes were titrated with increasing amounts of CT-

DNA. Excitation wavelength of the samples were 338 nm, scan speed=240 nm/min, slit width 10/10 nm. All experiments were conducted at 20 $^\circ\text{C}$ in a buffer containing 5 mM Tris–HCl (pH 7.2) and 50 mM NaCl concentrations.

Viscosity experiments were conducted on an Ubbelodhe viscometer, immersed in a thermostatted water-bath maintained at 25 ± 0.1 $^\circ\text{C}$. Data were presented as $(\eta/\eta_0)^{1/3}$ versus the ratio of the concentration of the compound to CT-DNA, where η is the viscosity of CT-DNA in the presence of the compound and η_0 is the viscosity of CT-DNA alone. Viscosity values were calculated from the observed flow time of CT-DNA containing solutions corrected from the flow time of buffer alone (t_0), $\eta = t - t_0$ [18].

The CD (circular dichroic) spectra were recorded on an Olos RSM 1000 at increasing complex/DNA ratio ($r=0.0, 0.5$). Cyclic voltammetry experiments were performed at room temperature under an inert atmosphere (N_2) with a conventional three-electrode electrochemical cell, and using a CHI-420 electrochemical workstation (made in Shanghai, China).

In antioxidant activity experiments the superoxide radicals ($\text{O}_2^{\bullet-}$) were generated in vitro by non-enzymatic system and determined spectrophotometrically by nitro blue tetrazolium (NBT) photoreduction method with a little modification in the method adopted elsewhere [19, 20]. The amount of $\text{O}_2^{\bullet-}$ and suppression ratio for $\text{O}_2^{\bullet-}$ can be calculated by measuring the absorbance at 560 nm. Solution of MET, VitB₂ and NBT were prepared at avoiding light. The tested compounds were dissolved in DMF (*N,N*-dimethylformamide). The assay mixture, in a total volume of 5 ml, contained MET (10 mM), NBT (46 μM), VitB₂ (3.3 μM), the tested compound (10–30 μM) and a phosphate buffer (67 mM, pH 7.8). After illuminating with a fluorescent lamp at 30 $^\circ\text{C}$ for 10 min, the absorbance of the samples (A_i) was measured at 560 nm. The sample without the tested compound was used as control and its absorbance was A_0 . All experimental results were expressed as the mean \pm standard deviation (S.D.) of triplicate determinations. The suppression ratio for $\text{O}_2^{\bullet-}$ was calculated from the following expression:

$$\text{Suppression ratio (\%)} = A_0 - A_i/A_0 \times 100 \quad (2)$$

Drug activity was expressed as the 50% inhibitory concentration (IC_{50}). IC_{50} values were calculated from regression lines where: x was the tested compound concentration in mM and y was percent inhibition of the tested compounds.

In antioxidant activity experiments the hydroxyl radicals (OH^\bullet) in aqueous media were generated through the Fenton system [21]. The solution of the tested compound was prepared with DMF. The 5 ml assay mixture contained following reagents: safranin (11.4 μM), EDTA–Fe(II) (40 μM), H_2O_2 (1.76 mM), the tested compound (10–

30 μ M) and a phosphate buffer (67 mM, pH 7.4). The assay mixtures were incubated at 37 °C for 30 min in a waterbath. After which, the absorbance was measured at 520 nm. All the tests were run in triplicate and expressed as the mean \pm standard deviation (S.D.).

The suppression ratio for OH \cdot was calculated from the following expression:

$$\text{Suppression ratio (\%)} = [(A_i - A_0)/(A_c - A_0)] \times 100 \quad (3)$$

(where A_i =the absorbance in the presence of the tested compound; A_0 =the absorbance in the absence of the tested compound; A_c =the absorbance in the absence of the tested compound, EDTA–Fe(II), H₂O₂.)

Preparation of the ligand (H₂L)

The preparation of the ligand is shown in Fig. 1. A mixture of *p*-Toluene Sulfonamide (5.14 g, 0.03 mol) and finely pulverized K₂CO₃ (11 g, 0.078 mol) in 35 ml of acetone was stirred and heated to reflux for 30 min. Acetone solution (10 ml) of ethyl chloroformate (3.8 ml, 0.04 mol) was added neat to the refluxing mixture. The mixture of the results were poured into 100 ml of H₂O, then the aqueous phases was acidified with 10 ml of 1.0 N aqueous HCl to get the solid, washed with 80 ml H₂O for several times. Recrystallization from 20 ml ethanol provided 6.35 g (87%) of ethyl *N*-(3-tossulfonyl) carbamate as a white crystalline solid.

A solution of ethyl *N*-(3-tossulfonyl) carbamate (730 mg, 3 mmol) and 4-aminoantipyrene (589 mg, 2.9 mmol) in 20 ml acetonitrile was heated to reflux for 10 h. After the solution stood overnight at room temperature, the resulting precipitate was collected, washed twice time with acetonitrile. Recrystallisation from 1:1 (v/v) acetonitrile/H₂O gave the ligand, which was dried in vacuum to afford 960 mg (89%) of a white solid: mp 182–184 °C; ¹H NMR (DMSO-*d*₆) δ 2.05 (bm, 4H), 2.36 (s, 3H), 3.00 (s, 3H), 7.30–7.28 (m, 3H), 7.52–7.37 (m, 4H),

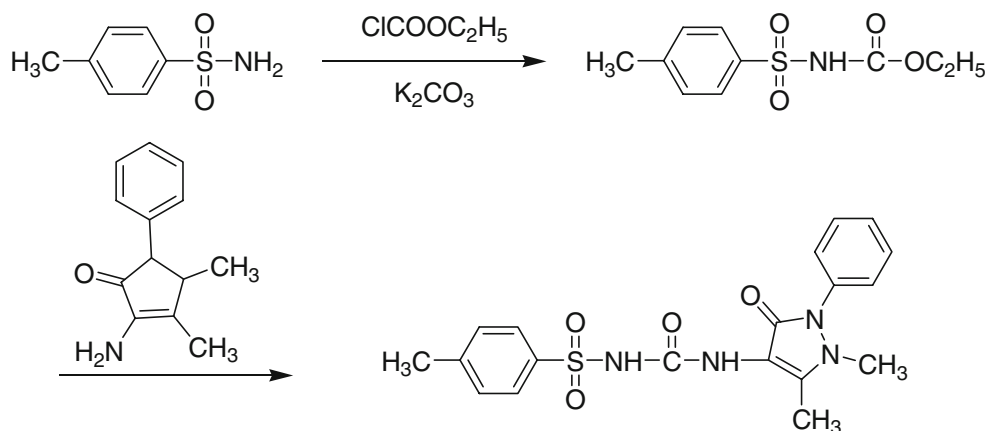
7.62 (bs, 1H), 7.79–7.85 (m, 2H), 11.44 (bs, 1H). FAB-MS: m/z =401 [M+H]⁺. Anal. Calcd for C₂₀H₂₁N₃O₄S: C, 56.99; H, 5.03; N, 13.99. Found: C, 56.81; H, 4.95; N, 14.06. IR ν_{\max} (cm⁻¹): $\nu_{\text{(aminoantipyrene)}}$ (C=O): 1,719 cm⁻¹, $\nu_{\text{(carbonyl)}}$ (C=O): 1,628 cm⁻¹, $\nu_{\text{(SOONH-)}}$ (N–H): 3,728 cm⁻¹. U_{\max} : (nm) 205, 227.

Preparation of the complexes

The Nd(NO₃)₃·6H₂O (219.1 mg, 0.5 mmol) in ethanol (10 ml) was added to the solution containing the ligand (200 mg, 0.5 mmol) in ethanol (10 ml). The mixture was stirred. After 24 h, the precipitate of Nd(III) complex formed. The precipitate was separated by the centrifugal and washed seven times with ethanol and one time with ether, and finally dried in vacuo. The Sm (III) and Eu(III) complexes were synthesized by the same way. Anal. Calcd for complex **1** C₆₀H₆₃N₁₂O₂₁S₃Nd: C, 47.28 (47.14); H, 4.17 (4.15); N, 11.21 (11.00); Nd, 9.38 (9.44).

A_m (s cm² mol⁻¹): 221.6. ESI-MS [CH₃OH, m/z]: 1,526.3 ([Nd(H₂L)₃·3NO₃]+H)⁺, 1,337.2 ([Nd(H₂L)₃·3NO₃]-3NO₃-2H)⁺, 940.2 ([Nd(H₂L)₃·3NO₃]-3NO₃-H₂L-2H)⁺, 540.1 ([Nd(H₂L)₃·3NO₃]-3NO₃-2H₂L-2H)⁺. IR ν_{\max} (cm⁻¹): $\nu_{\text{(aminoantipyrene)}}$ (C=O): 1,700 cm⁻¹, $\nu_{\text{(carbonyl)}}$ (C=O): 1,615 cm⁻¹, $\nu_{\text{(SOONH-)}}$ (N–H): 3,727 cm⁻¹. U_{\max} : (nm) 205, 227, 272. Anal. Calcd for complex **2** C₆₀H₆₃N₁₂O₂₁S₃Sm: C, 46.88 (46.95); H, 4.25 (4.14); N, 10.88 (10.95); Sm, 9.86 (9.80). A_m (s cm² mol⁻¹): 223.7. ESI-MS [CH₃OH, m/z]: 1,531.3 ([Sm(H₂L)₃·3NO₃]+H)⁺, 1,347.3 ([Sm(H₂L)₃·3NO₃]-3NO₃-2H)⁺, 950.3 ([Sm(H₂L)₃·3NO₃]-3NO₃-H₂L-2H)⁺, 550.1 ([Sm(H₂L)₃·3NO₃]-3NO₃-2H₂L-2H)⁺. IR ν_{\max} (cm⁻¹): $\nu_{\text{(aminoantipyrene)}}$ (C=O): 1,700 cm⁻¹, $\nu_{\text{(carbonyl)}}$ (C=O): 1,613 cm⁻¹, $\nu_{\text{(SOONH-)}}$ (N–H): 3,728 cm⁻¹. U_{\max} : (nm) 205, 227, 272. Anal. Calcd for complex **3** C₆₀H₆₃N₁₂O₂₁S₃Eu: C, 46.85 (46.91); H, 4.19(4.13); N, 10.87 (10.94); Eu, 9.77 (9.89). A_m (s cm² mol⁻¹): 226.8. ESI-MS [CH₃OH, m/z]: 1,537.3 ([Eu(H₂L)₃·3NO₃]+H)⁺, 1,348.3 ([Eu

Fig. 1 The preparation of the ligand



(H_2L) $_3\cdot 3\text{NO}_3$ – 3NO_3 – 2H^+), 951.2 ($\{[\text{Eu}(\text{H}_2\text{L})_3\cdot 3\text{NO}_3] - 3\text{NO}_3 - \text{H}_2\text{L} - 2\text{H}^+\}$), 551.1 ($\{[\text{Eu}(\text{H}_2\text{L})_3\cdot 3\text{NO}_3] - 3\text{NO}_3 - 2\text{H}_2\text{L} - 2\text{H}^+\}$). IR ν_{max} (cm^{-1}): $\nu_{(\text{aminoantipyrine})}$ (C=O): 1,701 cm^{-1} , $\nu_{(\text{carbonyl})}$ (C=O): 1,615 cm^{-1} , $\nu_{(-\text{SOONH}-)}$ (N–H): 3,726 cm^{-1} . U_{max} : (nm) 205, 227, 272.

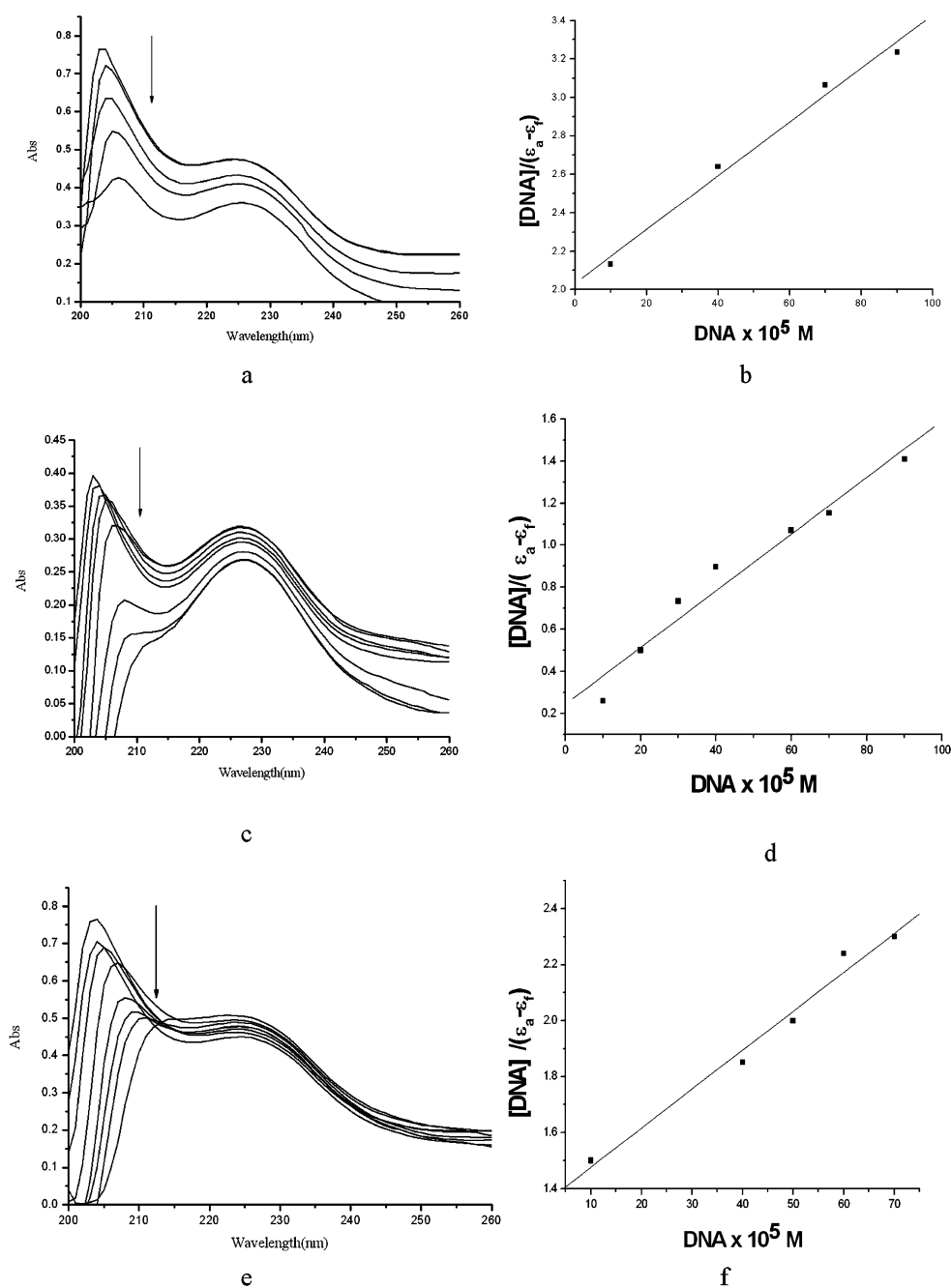
Results and discussion

All of the complexes are air stable for extended periods and remarkably soluble in DMSO and DMF; soluble in methanol and slightly soluble in ethanol; insoluble in

benzene, water and diethyl ether, and can be kept in air for a long time.

The structures of the complexes were characterized by elemental analyses, molar conductivities and IR spectra. The elemental analyses show that the formulas of the complexes conform to $\text{M}(\text{H}_2\text{L})_3\cdot 3\text{NO}_3$ ($\text{M}=\text{Nd}, \text{Sm}, \text{Eu}$) [where $\text{M}=\text{Nd}(\text{III}), \text{Sm}(\text{III})$ and $\text{Eu}(\text{III})$; H_2L is the ligand 1-(4-aminoantipyrine)-3-tosylurea]. The molar conductivities in DMF solution indicate that the $\text{Nd}(\text{III})$ complex (**1**), $\text{Sm}(\text{III})$ complex (**2**) and $\text{Eu}(\text{III})$ complex (**3**) (221.6, 223.7 and 226.8 $\text{S cm}^2 \text{mol}^{-1}$) are in the range expected for 3:1 electrolytes [22].

Fig. 2 Electronic spectra of the complex **1** (a), **2** (c), **3** (e) (10 μM) in the presence of 0, 20, 40, 60, and 80 μl 1.0×10^{-3} M CT-DNA. Arrow shows the emission intensities changes upon increasing DNA concentration. Inset plots of $[\text{DNA}]/(\epsilon_a - \epsilon_f)$ vs. $[\text{DNA}]$ for the titration of complex **1** (b), **2** (d), **3** (f) with DNA



Infrared spectra

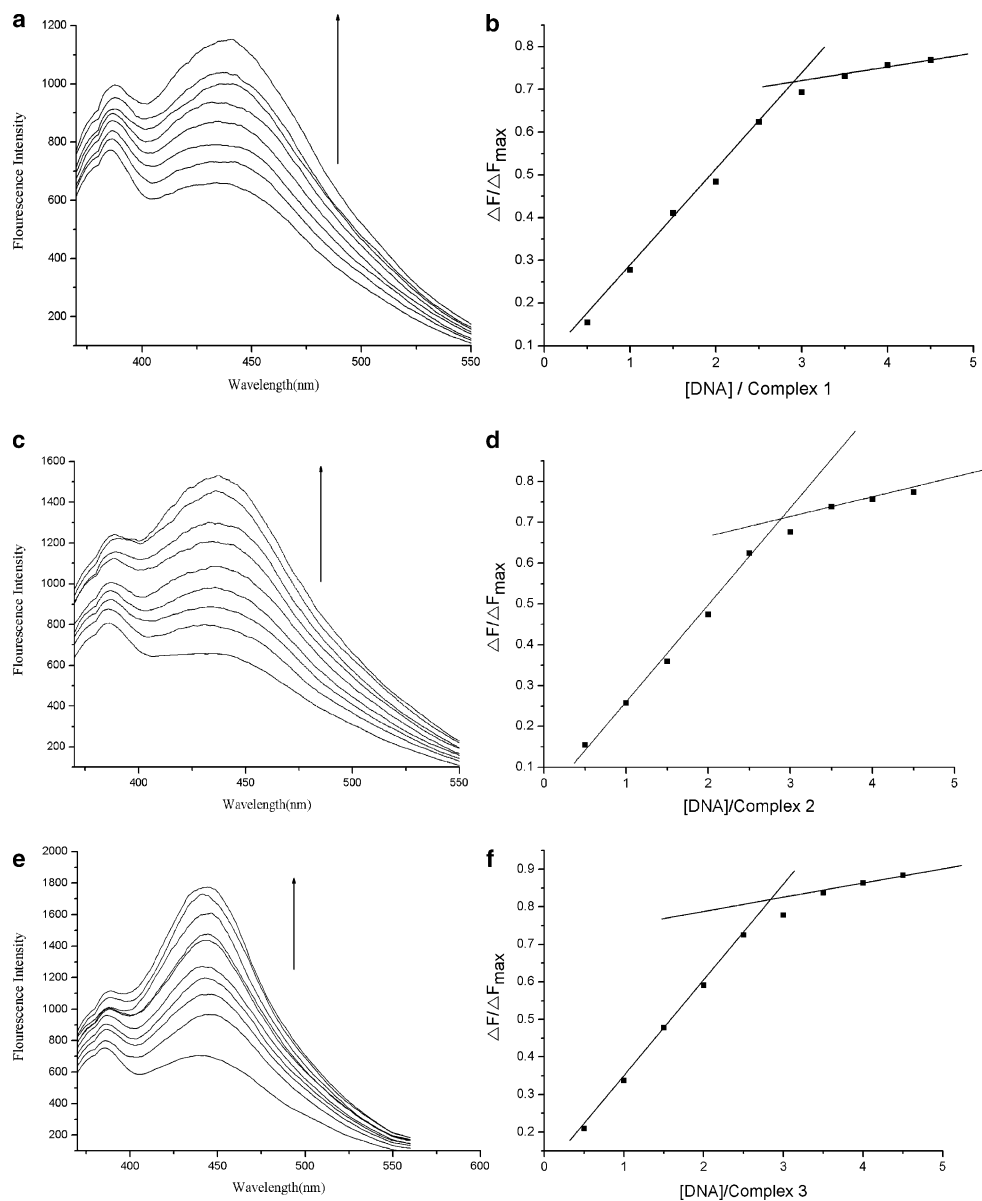
The IR spectra of the complexes are similar. The $\nu_{(\text{aminoantipyrine})} (\text{C}=\text{O})$ and $\nu_{(\text{carbonyl})} (\text{C}=\text{O})$ vibrations of the free ligand are at 1,719 and 1,628 cm^{-1} , respectively; for the complexes these peaks shift to 1,700 and 1,615 cm^{-1} , $\Delta\nu_{(\text{ligand-complexes})}$ is equal to 19 and 13 cm^{-1} . The band at the 1,316 cm^{-1} was $\nu_{(\text{SO}_2-)}$ vibration in the ligand. In the complexes this band is presented at 1,295 cm^{-1} , $\Delta\nu_{(\text{ligand-complexes})}$ is to 21 cm^{-1} . These data indicate that the oxygen of the carbonyl has likely formed a coordination bond with the rare earth ion [23]. In the complexes, the band at 579 cm^{-1} or so is assigned to $\nu(\text{M}-\text{O})$. These shifts demonstrate that the ligand coordinated Nd^{3+} , Sm^{3+} and

Eu^{3+} ions through the oxygen of carbonyl and sulphanilamide. The absorption band near 1,384 cm^{-1} indicates that free nitrate is also present [24].

UV–vis spectra

The study of the electronic spectra in the ultraviolet and visible ranges for the complexes and the ligand were carried out in the buffer solution. The electronic spectra of ligand had a strong band at $\lambda_{\text{max}}=205$ nm, a medium band at $\lambda_{\text{max}}=227$ nm. The complexes also yield two bands. A new band appeared at 272 nm for complex 1, 2 and complex 3. These changes indicate that complexes are formed.

Fig. 3 The fluorescence spectra of complex 1 (a), 2 (c), 3 (e) (10 μM) in the presence of 0, 20, 40, 60, 70, 80, 90 and 100 μl 1.0×10^{-3} M CT-DNA. Arrow shows the emission intensities changes upon increasing DNA concentration. Inset fluorescence binding isotherms for the association of complex 1 (b), 2 (d), 3 (f) with DNA. The binding stoichiometry in terms of number of nucleotide bases/drug molecule is the value at the intersection of the two straight lines



DNA-binding studies

UV absorption titration

The application of UV absorption spectroscopy in DNA-binding studies is one of the most useful techniques [25]. The absorption spectra of the complex **1**, complex **2** and **3** in the absence and presence of CT-DNA (at a constant concentration of complexes) are given in Fig. 2. In the presence of DNA, the absorption bands of **1**, **2** and **3** at about 205 nm exhibited hypochromism of about 18.9%, 20.2% and 35.1% and bathochromism of about 3, 5 and 7 nm. The spectroscopic changes suggest that the complexes have stronger interaction with DNA. The intrinsic binding constants K_b of complexes **1**, complex **2** and **3** were 3.18×10^5 , 5.51×10^5 and $9.63 \times 10^5 \text{ M}^{-1}$, respectively. The results indicate that the binding strength of complex **3** is stronger than that of complex **1** and **2**. The K_b value obtained here is lower than that reported for classical intercalator (for ethidium bromide and [Ru(phen)DPPZ] whose binding constants have been found to be in the order of 10^6 – 10^7 M^{-1}) [26, 27]. Such a small change in λ_{max} and the observed binding constant is more in keeping with the groove binding with DNA, as observed in the literature [28].

Fluorescence spectra studies

Complex **1**, complex **2** and **3** can emit fluorescence in Tris buffer at ambient temperature, with a maximum appearing at about 441 nm for complex **1**, complex **2** and **3**. As shown in Fig. 3, the fluorescence intensity of the complexes are

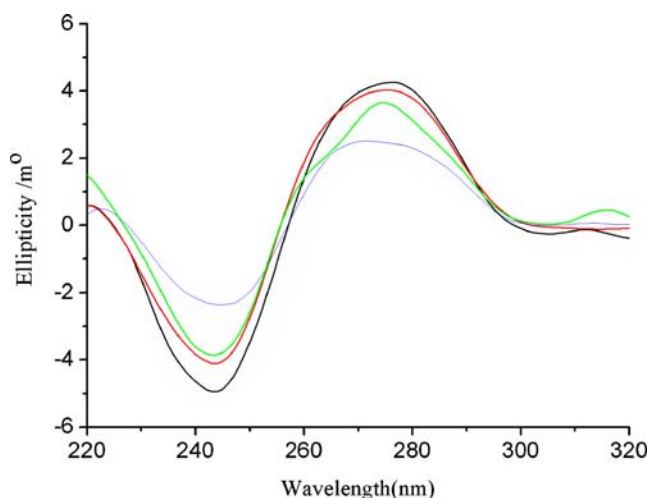


Fig. 4 CD spectrum of CT-DNA adduct with compound. Black line free CT-DNA, red line complex **1** with CT-DNA, $r_i=0.5$. (r_i =molar ratio compound: CT-DNA) Green line complex **2** with CT-DNA, $r_i=0.5$; blue line complex **3** with CT-DNA, $r_i=0.5$. (r_i =molar ratio compound: CT-DNA)

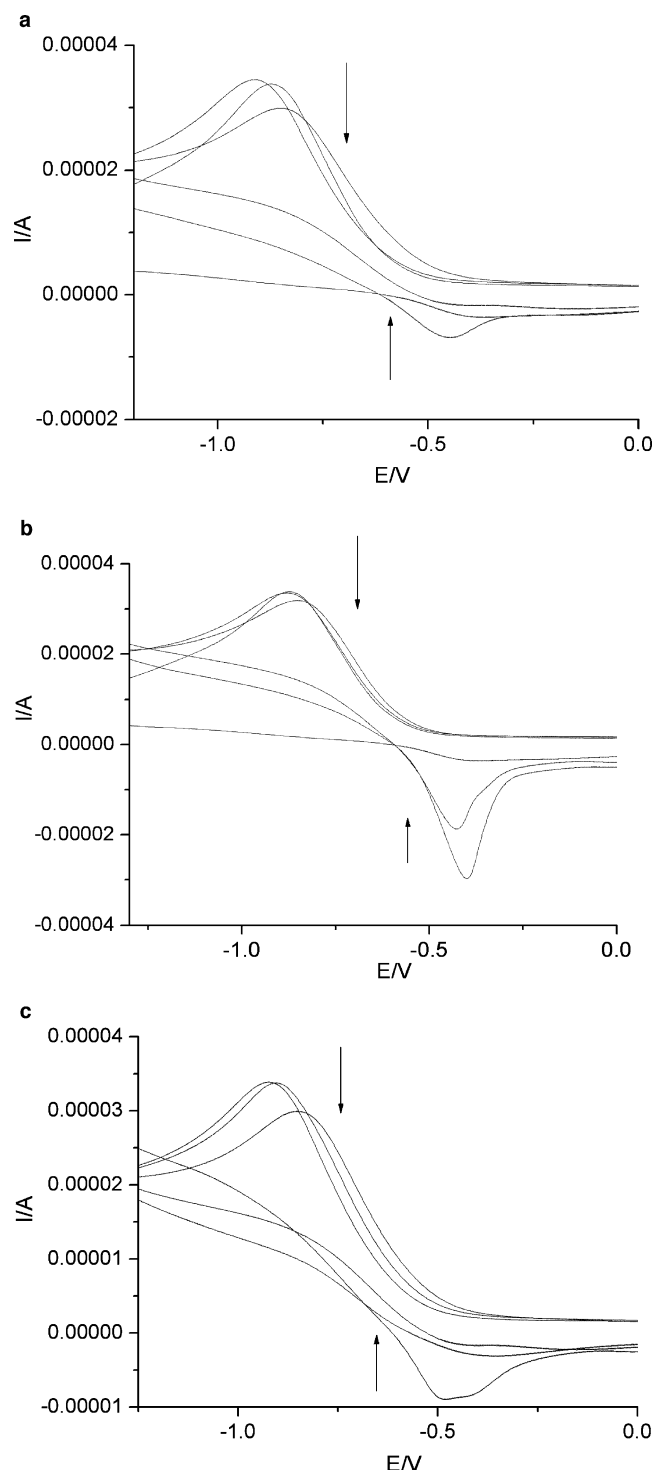


Fig. 5 Cyclic voltammogram of 0.50 mM complex **1** (a), complex **2** (b) and **3** (c). Supporting electrolyte, 100 mM NaClO_4 in DMF, Sweep rate, 50 mV/s. Arrow shows the current and potential changing upon increasing DNA concentrations. (**1**=0, 0.02, 0.03 mM DNA), (**2**=0, 0.01, 0.02, 0.03 mM DNA) and (**3**=0, 0.02, 0.03 mM DNA)

increased steadily with the increasing concentration of the CT-DNA, and emission maximum shift by 3 nm to longer wavelength (445 nm) for complex **1** and **2**, and no shift for **3**. This effect arises, in the presence of DNA, the metal

complex is bound in a relatively non-polar environment compared to water. The increase in the fluorescence intensity is less than that for the intercalators. The binding site size was determined from the binding stoichiometry of the complex-DNA isotherm as shown in Fig. 3. Knowledge about the binding stoichiometry of the metal-sulfonylurea-DNA complex would be helpful in characterizing the geometry of the drug binding to DNA. The intersection point of the binding isotherm, gives a binding site size of 8 bp per bound complex molecule. The binding site size allows one to distinguish between intercalating and non-intercalating binding agents [29]. Molecules showing large binding site sizes are indicative of non-intercalation as a probable mode of binding and they require correspondingly lower concentrations to saturate the sites. The binding isotherm of complex 1, complex 2 and 3 is again indicative of non-intercalative binding of the complexes to DNA.

CD spectroscopy

Circular dichroic spectral techniques give us useful information on how the conformation of DNA is influenced by the binding of the metal complex to DNA. The observed CD spectrum of calf thymus DNA consists of a positive band at 277 nm due to base stacking and a negative band at 245 nm due to helicity, which is characteristic of DNA in the right-handed B form. While groove binding and electrostatic interaction of small molecules with DNA show little or no perturbations on the base stacking and helicity bands, intercalation enhances the intensities of both the bands, stabilizing the right-handed B conformation of CT-DNA. The CD spectra of DNA taken after incubation of the complexes with CT DNA are shown in Fig. 4. In all three cases, the intensities of both the negative and positive bands decrease significantly. This suggests that the DNA binding of the complexes induces certain conformational changes, such as the conversion from a more B-like to a more C-like structure within the DNA molecule [30–32]. These changes

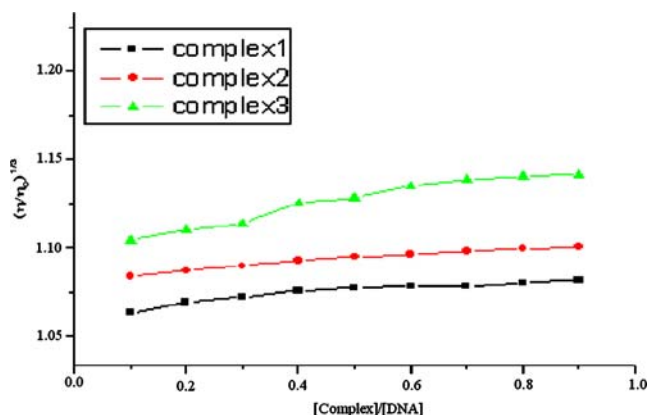


Fig. 6 Effect of increasing amounts of the complexes on the relative viscosity of CT-DNA at 25.0±0.1 °C

are indicative of a non-intercalative mode of binding of these complexes and offer support to their groove binding nature [33]. The changing intensity follow the order of 3>2>1.

Cyclic voltammetry

The application of electrochemical methods to the study of metalintercalation and coordination of metal complexes to

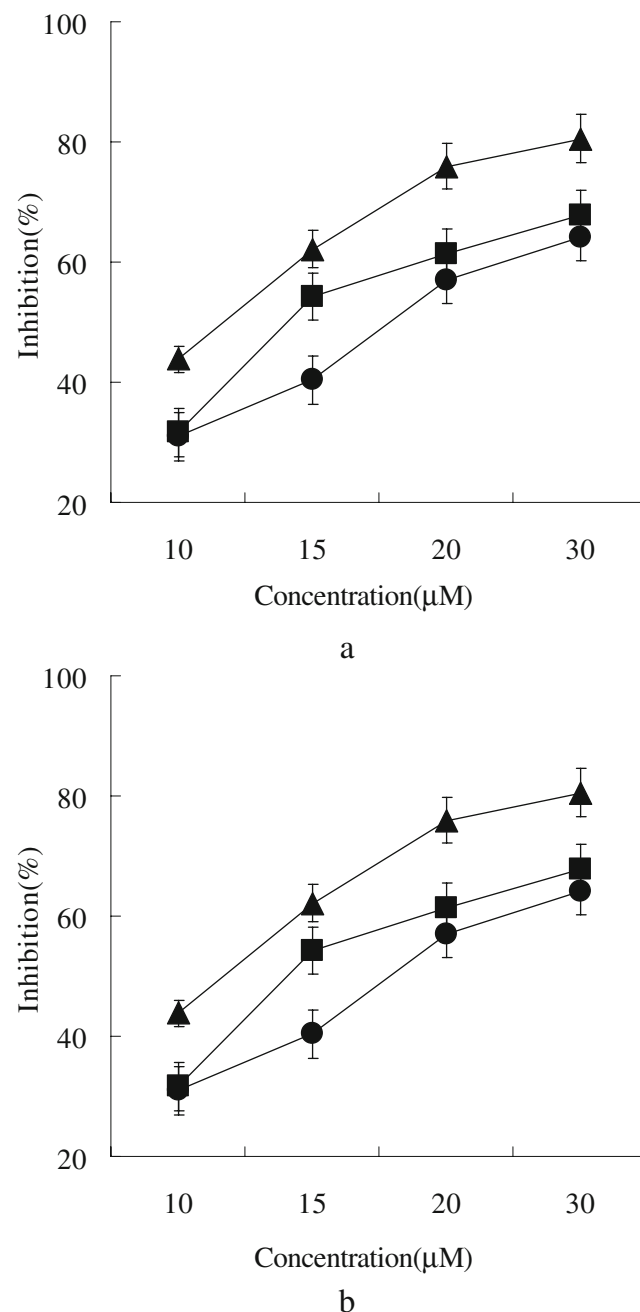


Fig. 7 **a** Effect of tested compounds on $O_2^{\bullet-}$. **b** Effect of tested compounds on OH^{\bullet} . Filled circles complex 1, filled squares complex 2, filled triangles complex 3. Experiments were performed in triplicate. Values are expressed as mean±standard deviation ($n=3$)

DNA provides a useful complement to the previously used methods of investigation, such as UV–Vis spectroscopy [34, 35]. Figure 5 shows the cyclic voltammograms of the complexes at the absence and presence of DNA. It can be seen that the cathode and anode peak currents decreased gradually with the addition of DNA. The decrease in current may be attributed to the diffusion of the complexes bound to the large, slowly diffusing DNA molecule. The decreases in the peak currents are ascribed to the stronger binding between the complexes and DNA. In addition, the peak potentials, E_{pc} and E_{pa} , as well as $E_{1/2}$ had a shift to more positive potential. The shift of the redox potential of the complexes in the presence of DNA to more positive values indicates a binding interaction between the complex and DNA that makes the complexes readily reducible. The decreased extents of the peak currents observed for the complexes upon addition of CT-DNA may indicate that complex **3** possesses higher DNA-binding affinity than complex **1** and **2** do. The results parallel the above spectroscopic and viscosity data of Nd, Sm and Eu complexes in the presence of DNA.

Viscosity studies

Optical photophysical probes generally provide necessary, but not sufficient clues to support a binding model. Measurements of DNA viscosity that is sensitive to DNA length are regarded as the least ambiguous and the most critical tests of binding in solution in the absence of crystallographic structural data [36, 37]. Intercalating agents are expected to elongate the double helix to accommodate the ligands in between the base leading to an increase in the viscosity of DNA. In contrast, complex that bind exclusively in the DNA grooves by partial and/or non-classical intercalation, under the same conditions, typically cause less pronounced (positive or negative) or no change in DNA solution viscosity [38]. The values of $(\eta/\eta_0)^{1/3}$ were plotted against [complex]/[DNA] (see Fig. 6). The results reveal that the complex **1**, complex **2** and **3** effect relatively inapparent increase in DNA viscosity, which is consistent with DNA groove binding suggested above, which is also known to enhance DNA viscosity [39]. The increased degree of viscosity, which may depend on its affinity to DNA follows the order of **3**>**2**>**1**, which is consistent with our foregoing hypothesis.

Antioxidant activity

Figure 7 depicts the inhibitory effect of the complexes on $O_2^{\bullet -}$ and OH^{\bullet} . The antioxidant activities of these compounds are expressed as 50% inhibitory concentration (IC_{50} in μM). IC_{50} values of **1**, **2** and **3** are 19.6 ± 0.25 , 15.3 ± 0.13

and 12.5 ± 0.12 μM , respectively. The compound **3** shows better inhibitory effect than **2** and **1**. We can also find that all compounds scavenge OH^{\bullet} also in a concentration-dependent manner. The complexes show highly active scavenging effect on OH^{\bullet} . The suppression ration take the order of **3**>**2**>**1**.

It is clear that the scavenger effect on $O_2^{\bullet -}$ can be by the formation of metal–ligand coordination complexes and the nature of the rare earth ions also affects the ability. Some complexes we have synthesized are better effective inhibitor for $O_2^{\bullet -}$ than that of the nitroxide Tempo ($IC_{50} = 60 \pm 3.11$ M) which has been recently used in biological system for its capacity to mimic superoxide dismutase [40, 41]. Although superoxide is a relatively weak oxidant, it decomposes to form stronger relative oxidative species, such as single oxygen and hydroxyl radicals, which initiate peroxidation of lipids [42]. In the present study, the complexes effectively scavenged superoxide in a concentration-dependent manner. These results showed the complexes have significant scavenging activity of superoxide radical and clearly suggested that the antioxidant activity of the complexes was also related to its ability to scavenge superoxide radical.

It is clearly shown that metal complexes exhibit considerable scavenging activity due to the chelation of organic molecule to rare earth ions and rare earth ions such as La (III), Sm(III), Eu(III) and Dy(III) exert differential and selective effects on scavenging radicals of the biological system. Moreover, we find that these complexes are better effective inhibitor for OH^{\bullet} than that of mannitol which is usually used as special scavenger for OH^{\bullet} . Therefore, the metal complexes we studied in this paper deserve to be further researched.

Conclusions

Taken together, a new ligand, 1-(4-aminoantipyrine)-3-tosylurea (H_2L), and its lanthanide (III) complexes have been prepared and characterized. The DNA-binding properties of the complex **1**, complex **2** and **3** were investigated by UV–vis absorption and fluorescence and CD spectra, CV and viscosity measurements. Experimental results indicate that the complexes can bond to CT-DNA take the mode of groove binding, and complex **3** have stronger binding affinity than complex **1** and **2**. Furthermore, the three rare earth complexes have active scavenging effect on $O_2^{\bullet -}$ and OH^{\bullet} . These findings clearly indicate that lanthanide-based complexes have many potential practical applications, like the development of nucleic acid molecular probes and new therapeutic reagents for diseases.

Acknowledgments This project was supported by the National Natural Science Foundation in China (20171019) and Zhide Foundation.

References

- Brown GR, Foubister AJ (1984) Receptor binding sites of hypoglycemic sulfonylureas and related [(acylamino)alkyl]benzoic acids. *J Med Chem* 27:79–81
- Rufer C, Biere H, Ahrens H, Loge O, Schroder E (1974) Blood glucose lowering sulfonamides with asymmetric carbon atoms. 1. *J Med Chem* 17:708–715
- Howbert JJ, Grossman CS, Crowell TA (1990) Novel agents effective against solid tumors: the diarylsulfonylureas. Synthesis, activities, and analysis of quantitative structure–activity relationships. *J Med Chem* 33:2393–2407
- Xu H, Liang Y, Zhang P, Pu F, Zhou BR, Wu J, Liu JH, Liu ZG, Gao L, Ji LN (2005) Biophysical studies of a ruthenium(II) polypyridyl complex binding to DNA and RNA prove that nucleic acid structure has significant effects on binding behaviors. *J Biol Inorg Chem* 10:529–538
- Williams DR (1972) Metals, ligands and cancer. *Chem Rev* 72:203–213
- Grindey GB (1990) Current status of cancer drug development: failure or limited success. *Cancer Cells* 2:163–171
- Zhang SC, Zhu YG, Tu C, Wei HY, Yang Z, Lin LP, Ding J, Zhang JF, Guo ZJ (2004) A novel cytotoxic ternary copper(II) complex of 1,10-phenanthroline and L-threonine with DNA nuclease activity. *J Inorg Biochem* 98:2099–2106
- Mohamadi FB, Spees MM, Grindey GB (1992) Sulfonylureas: a new class of cancer chemotherapeutic agents. *J Med Chem* 35:3012–3016
- Eriksson M, Leijon M, Hiort C, Norden B, Gradsland A (1994) Binding of delta- and lambda-[Ru(phen)₃]²⁺ to [d(CGCG ATCGCG)]₂ Studied by NMR. *Biochemistry* 33:5031–5040
- Scatchard G (1949) The attractions of proteins for small molecules and ions. *Ann NY Acad Sci* 51:660–672
- Martin RB, Richardson FS (1979) Lanthanides as probes for calcium in biological systems. *Q Rev Biophys* 12:181–209
- Laufer RB (1987) Paramagnetic metal complexes as water proton relaxation agents for NMR imaging: theory and design. *Chem Rev* 87:901–927
- Shibasaki M, Sasai H, Arai T (1997) Asymmetric catalysis with heterobimetallic compounds. *Angew Chem Int Ed Engl* 36:1236–1256
- Xi PX, Liu XH, Lu HL, Zeng ZZ (2007) Synthesis, characterization and DNA-binding studies of 1-(pyridin-2-yl)-3-tosylurea and its Nd(III), Eu(III) complexes. *Transit Met Chem* 32:757–761
- Satyanarayana S, Dabrowiak JC, Chaires JB (1993) Tris(phenanthroline)ruthenium(II) enantiomer interactions with DNA: mode and specificity of binding. *Biochemistry* 32:2573–2584
- Marmur J (1961) A procedure for the isolation of deoxyribonuclei from micro-organisms. *J Mol Biol* 3:208–218
- Pyle AM, Rehmann JP, Meshoyrer R, Kumar CV, Turro NJ, Barton JK (1989) Mixed-ligand complexes of ruthenium(II): factors governing binding to DNA. *J Am Chem Soc* 111:3051–3058
- Michael TC, Marisol R, Allen JB (1989) Voltammetric studies of the interaction of metal chelates with DNA. 2. Tris-chelated complexes of cobalt(III) and iron(II) with 1,10-phenanthroline and 2,2'-bipyridine. *J Am Chem Soc* 111:8901–8911
- Kumar CV, Asuncion EH (1993) DNA binding studies and site selective fluorescence sensitization of an anthryl probe. *J Am Chem Soc* 115:8547–8553
- Winterbourn CC (1979) Comparison of superoxide with other reducing agents in the biological production of hydroxyl radicals. *Biochem J* 182:625–628
- Winterbourn CC (1981) Hydroxyl radical production in body fluids: roles of metal ions, ascorbate and superoxide. *Biochem J* 198:125–131
- Geary WJ (1971) The use of conductivity measurements in organic solvents for the characterization of coordination compounds. *Coord Chem Rev* 7:81–122
- Wang Y, Yang ZY, Wang Q, Cai QK, Yu KB (2005) Crystal structure, antitumor activities and DNA-binding properties of the La(III) complex with Phthalazin-1(2H)-one prepared by a novel route. *J Organomet Chem* 690:4557–4563
- Nakamoto K (1978) Infrared and Raman spectra of inorganic and coordination compound, 3rd edn. Wiley-Interscience, New York
- Barton JK, Danishefsky AT, Goldberg JM (1984) Tris(phenanthroline)ruthenium(II): stereoselectivity in binding to DNA. *J Am Chem Soc* 106:2172–2176
- Cory M, McKee DD, Kagan J, Henry DW, Miller JA (1985) Design, synthesis, and DNA binding properties of bifunctional intercalators. Comparison of polymethylene and diphenyl ether chains connecting phenanthridine. *J Am Chem Soc* 107: 2528–2536
- Waring MJ (1965) Complex formation between ethidium bromide and nucleic acids. *J Mol Biol* 13:269–282
- Vaidyanathan VG, Nair BU (2003) Photooxidation of DNA by a cobalt (II) tridentate complex. *J Inorg Biochem* 94:121–126
- Krishna AG, Kumar DV, Khan BM, Rawel SK, Ganesh KN (1998) Taxol–DNA interactions: fluorescence and CD studies of DNA groove binding properties of taxol. *Biochim Biophys Acta* 1381:104–112
- Vaidyanathan VG, Nair BU (2000) Interaction of DNA with [Cr (Schiff base)(H₂O)₂](ClO₄). *Biochim Biophys Acta* 1475:157–162
- Wang BD, Yang ZY, Qin DD, Chen ZN (2008) Synthesis, characterization, cytotoxic activity and DNA-binding properties of the Ln(III) complexes with ethylenediiminobi(6-hydroxychromone-3-carbaldehyde) Schiff-base. *J Photochem Photobiol A Chem* 194:49–58
- Song YM, Wu Q, Yang PJ, Luan NN, Wang LF, Liu YM (2006) DNA binding and cleavage activity of Ni(II) complex with all-trans retinoic acid. *J Inorg Biochem* 100:1685–1691
- Rajendran A, Nair BU (2006) Unprecedented dual binding behaviour of acridine group of dye: a combined experimental and theoretical investigation for the development of anticancer chemotherapeutic agents. *Biochim Biophys Acta* 1760:1794–1801
- Johnston DH, Thorp HH (1995) Electrochemical measurement of the solvent accessibility of nucleobases using electron transfer between DNA and metal complexes. *J Am Chem Soc* 117:8933–8938
- Indumathy R, Radhika S, Kanthimathi M, Weyhermuller T, Nair BU (2007) Cobalt complexes of terpyridine ligand: crystal structure and photocleavage of DNA. *J Inorg Biochem* 101:434–443
- Mesmaeker AD, Orellana G, Barton JK, Turro NJ (1990) Ligand-dependent interaction of Ruthenium(II) polypyridyl complexes with DNA probed by emission spectroscopy. *Photochem Photobiol* 52:461–472
- Lakowicz JR, Jayaweera R, Szmazinski H, Wiczak W (1989) Resolution of two emission spectra for tryptophan using frequency-domain phase-modulation spectra. *Photochem Photobiol* 10:541–546
- Chen R, Liu CS, Zhang H, Guo Y, Bu XH, Yang M (2007) Three new Cu(II) and Cd(II) complexes with 3-(2-pyridyl)pyrazole-based ligand: syntheses, crystal structures, and evaluations for bioactivities. *J Inorg Biochem* 101:412–421
- Selvi PT, Palaniandavar M (2002) Spectral, viscometric and electrochemical studies on mixed ligand cobalt(III) complexes of certain diimine ligands bound to calf thymus DNA. *Inorg Chim Acta* 337:420–428

40. Samuni A, Krisna MC (1997) In: Packer L, Cadenas E (eds) Handbook of synthetic antioxidants (chapter: Antioxidant properties of nitroxides and nitroxide SOD mimics); New York, pp 351–373
41. Xi PX, Xu ZH, Liu XH, Chen FJ, Huang L, Zeng ZZ (2008) Synthesis, characterization, antioxidant activity, and DNA-binding studies of 1-cyclohexyl-3-tosylurea and its Nd(III), xEu(III) complexes. *Chem Pharm Bull* 56:541–546
42. Wang BD, Yang ZY, Crewdson P, Wang DQ (2007) Synthesis, crystal structure and DNA-binding studies of the Ln(III) complex with 6-hydroxychromone-3-carbaldehyde benzoyl hydrazone. *J Inorg Biochem* 101:1492–1504